Dynamic interaction between adjacent buildings through nonlinear soil during earthquakes

Felipe Vicencio [a*], Nicholas A. Alexander [b].

[a] *Researcher, Department of Civil Engineering, University of Bristol, Queen's Building, Bristol, UK*
[b] *Senior Lecturer in Structural Engineering, Department of Civil Engineering, University of Bristol, Queen's Building, Bristol, UK*

Abstract

This paper evaluates the effect of Structure-soil-structure interaction (SSSI) between two buildings given different parameters of the buildings, inter-building spacing, and soil type. A two-dimensional simple discrete nonlinear model is proposed that is described by a set of nonlinear differential equations of motion. A nonlinear phenomenological Bouc-Wen model, for the soil directly underneath the foundations, linear rotational interaction spring between buildings and linear behaviour of buildings are assumed. The seismic ground motion employed is spectrally matched with EC8 elastic spectra. The results showed that there are both unfavourable and beneficial configurations of the two buildings that produce important differences between nonlinear SSSI and nonlinear SSI (the uncoupled building case). Importantly it is demonstrated that the adverse effects of SSSI can be more pronounced when the nonlinear soil behaviour is assumed.

Keywords: Nonlinear analysis, Structure-soil-structure interaction, time history seismic analysis.

1. Introduction

Conventionally, buildings in urban areas are designed by considering the response of structures in isolation. However, the high density of buildings in cities inevitably results in the possibility of seismic interaction of adjacent buildings through the underlying soil. This phenomenon is widely known as structure-soil-structure interaction (SSSI) and has been reported in the pioneering works of Luco and Contesse [1], Kobori et al. [2], Lee and Wesley [3], Mattiesen and MacCalden [4], Wong and Trifunac [5], Lysmer et al. [6] and Roesset and Gonzales [7].

The importance of including the beneficial/adverse structural effects of the dynamic interaction between several structures has received sustained attention in recent years. Kitada et al. [8], Yano et al. [9], Hans et al. [10], Li et al. [11] are experimental in situ studies. Aldaikh et al. [12] performed a series of scale model shaking table test to study the effect of SSSI on the response of building with two or three adjacent buildings. Numerical studies based on finite element method (FEM), boundary elements method (BEM) or a combination of these two FEM/BEM procedures with Bard et al. [13], Yahyai et al. [14], Padron et al. [15], Bolisetti and Whittaker [16], Alexander et al. [17], Aldaikh et al. [18], Chouw and Schmid [47] and Ogut and Fukuwa [48].

These studies have highlighted the importance of considering the dynamic coupling between several structures, including the identification of key factors that may control the seismic behaviour and the amount of structural interactions such as, (i) the inter-building distance, (ii) the direction of the alignment between foundations, (iii) the relative height and dynamic characteristics of adjacent buildings, (iv) the aspect ratio between height to width of buildings and (v) the general soil class.

The interchange of energy between the soil and the structure during nonlinear dynamical responses is an important issue in earthquake engineering. Although the equivalent linear type of analysis is the most popular, they have some well-known limitations for the case of large magnitude earthquake excitation. Several

* Corresponding author. Tel.: +447517759978.
E-mail address: fv16607@bristol.ac.uk (F. Vicencio).

researchers [19-22] have extensively investigated soil-structure interaction (SSI) by explicitly considering the soil-foundation model through a nonlinear macro-element. However, this analysis does not consider the interaction of adjacent buildings via the underlying soil during an earthquake.

Nomenclature

α_1, α_2	ratio of foundation/soil to building masses of buildings 1 and 2 respectively []
β	ratio of soil/foundation radii of gyration for buildings 1 and 2 respectively []
ς_1, ς_2	parameter describing shape and amplitude of hysteresis buildings 1 and 2 respectively []
ψ_1, ψ_2	parameter describing shape and amplitude of hysteresis buildings 1 and 2 respectively []
γ_y	strain at initiation of nonlinear soil behaviour []
δ_η	Stiffness degradation factor []
δ_ν	Strength degradation factor []
ε	height ratio of buildings 2 to 1 []
η_1, η_2	height to radius of gyration ratios for buildings 1 and 2 respectively []
$\eta(E)$	stiffness degradation shape function of hysteresis model []
η_s	damping correction factor of the elastic spectrum []
θ_1, θ_2	rotation at base of buildings 1 and 2 respectively []
κ	rotational interaction spring between buildings 1 and 2 [ML^2T^{-2}]
λ	ratio of mass polar moments of inertia of soil-foundation of buildings 1 and 2 respectively []
μ	Poison's ratio of soil []
$\nu(E)$	strength degradation shape function of hysteresis model []
ξ_n	ratio of critical damping of soil beneath buildings []
ρ_b, ρ_s	densities (average) of building and soil respectively [ML^{-3}]
τ	scaled time []
$\boldsymbol{\phi}_n$	modal eigenvector of the linear system []
χ_{ii}	percentage change in total displacement power when moving from uncoupled to coupled state for building i
$\ddot{\chi}_{ii}$	percentage change in total acceleration power, moving from uncoupled to coupled state for building i [%]
ω_1, ω_3	modal circular frequency on rock of buildings 1 and 2 respectively [rad T^{-1}]
ω_2, ω_4	circular frequency of soil/foundation of buildings 1 and 2 respectively [rad T^{-1}]
ω	Fourier frequency [rad T^{-1}]
ω_n	natural frequencies of the linear systems [rad T^{-1}]
ϖ	interaction circular frequency ratio parameter [rad T^{-1}]
Ω_0	ratio of interaction to building 1 (on rock) circular frequencies []
Ω_2	ratio of building 1 (soil/foundation) to building 1 (on rock) circular frequencies []
Ω_3	ratio of building 2 (on rock) to building 1 (on rock) circular frequencies []
Ω_4	ratio of building 2 (soil/foundation) to building 1 (on rock) circular frequencies []
A_1, A_2	total non-dimensional acceleration of building 1 and 2 respectively []
a_g	peak ground acceleration of the elastic response spectrum [MT^{-2}]
a_{gr}	peak ground acceleration of the ground motion [MT^{-2}]
B_1, B_2	ratio of linear to nonlinear response of buildings 1 and 2 respectively []
b	foundation width []
$\boldsymbol{C}$	non-dimensional damping matrix []
c_1	density ratio (soil/buildings) parametric constant []
c_2	frequency ratio parametric constant []
D_1, D_2	parameter describing shape and amplitude of hysteresis buildings 1 and 2 respectively []
$E(\tau)$	dissipated hysteretic energy []
E_s	total power spectral density []
$\mathbf{f}$	non-dimensional force vector []
G_s	initial tangent shear modulus of the soil [$M\,L^{-1}T^{-2}$]
h_1, h_2	heights of building 1 and 2 respectively [L]
$\boldsymbol{K}$	non-dimensional stiffness matrix []
k_{b1}, k_{b2}	lateral modal stiffnesses of building 1 and 2 respectively [MT^{-2}]
k_{s1}, k_{s2}	rotational soil stiffnesses of soil beneath building 1 and 2 respectively [ML^2T^{-2}]
$\boldsymbol{M}$	non-dimensional mass matrix []
M_1, M_2	nonlinear moment due to the rotation and hysteretic rotation of buildings 1 and 2 respectively [ML^2T^{-2}]
M_s	surface wave magnitude scale
M_w	moment magnitude scale
m_{b1}, m_{b2}	modal masses of building 1 and 2 respectively [M]
m_{s1}, m_{s2}	soil/foundation masses underneath building 1 and 2 respectively [M]
n_1, n_2	parameter describing shape and amplitude of hysteresis buildings 1 and 2 respectively []
$Q_{ii}(\omega)$	power spectral density of total displacement of building i []
$\ddot{Q}_{ii}(\omega)$	power spectral density of total acceleration of building i []
q_1, q_2	non-dimensional nonlinear function of soil []
$\boldsymbol{q}$	non-dimensional nonlinear moment/rotation vector []
r_1, r_2	soil/foundation masses radius of gyration of building 1 and 2 respectively [L]
S_a	horizontal elastic response spectra [MT^{-2}]
s	aspect ratio – height to width of building 1 []
T_E	system kinematic energy [ML^2T^{-2}]
T_B, T_c, T_D	parameters that depends of the soil type, according to the elastic response spectra []
t	time [T]
U_1, U_2	total non-dimensional relative displacement to ground of building 1 and 2 respectively []
U_E	system potential energy [ML^2T^{-2}]
u_1, u_2	non-dimensional relative displacement to ground of building 1 and 2 respectively []
u_g	non-dimensional horizontal ground displacement time series []
$\boldsymbol{u}$	non-dimensional degree of freedoms vector []
V_s	shear wave velocity of soil [LT^{-1}]
$\bar{V}_s$	Normalised non-dimensional shear wave velocity of soil []
x_1, x_2	relative displacement to ground (in a rotating coordinate frame) of building 1 and 2 respectively [L]
x_g	horizontal ground displacement time series [L]
y_1, y_2	internal hysteretic rotations of buildings 1 and 2 respectively []
z	non-dimensional inter-building distance []

Experimental tests of specific building/foundation configurations, Trombetta et al. [50-52] and Mason et al. [53], model the nonlinear behaviour of soil and structure. These represent important validation points for numerical models. However, these experiments are technically challenging. This is because of the problem of scaling soil strains and inertial forces accurately. Additionally, they represent statistically, a small sample and hence provide only a limited parametric exploration of the problem. Some researcher's advocate using advanced computational models (FEA). Ghandil et al. [54] evaluate the SSSI in three different buildings, considering elasto-plastic frame hinges in the structure and two soils profile with a reduction of the soil shear modulus in areas close to the foundation. Bolisetti and Whittaker [55] study the SSSI in a nonlinear model developed in the time-domain code LS-DYNA. Specific cases can be modelled using this method. However, modelling a whole class of building configurations, in a large-scale parametric study, is very difficult in general. Thus, a large-scale parametric exploration of this problem requires a different method. The alternative is to use system models, with a relatively limited number of degrees of freedom, for a parametric study. These low-order models (i) capture the most significant dynamic behaviour, (ii) have a relatively small number of system parameters and (iii) are computationally simple enough for exploring a huge number of generic cases. This parametric studies should be viewed an initial exploration of the problem. They are not meant to replace advanced computational models and experimental work of specific cases.

1.1 Aims

In this paper, we extend our previous study on the SSSI of two linear buildings [17] to the case of nonlinear soil behaviour underneath buildings using the phenomenological Bouc-Wen model. In addition, we shall now employ seismic ground motion rather than Kanai-Tajimi artificial ground motion. In this new parametric study, we explore over 20000 different nonlinear systems. These span a range of geometric case with three different soil classes. This computationally challenging study required the High-Performance Computing (HPC) machine, BlueCrystal, at the University of Bristol. The code used in this study was developed in Matlab. The stiff nonlinear equations of motion for each model were solved using Matlab's ode15s (stiff ordinary differential equations) integrator [49]. To obviate the substantial computational costs we shall employ a single spectrally matched ground motion for the nonlinear time history analyses. Additionally, we considered the cases where inelastic behaviour occurs in the soil underneath the building's foundations rather than within the buildings. Thus, the building structures are considered to act linearly. The aim of this paper is to answer the following questions.

- Does the introduction of soil nonlinearity reduce the size of adverse/beneficial SSSI effects to a level at which it can be safely neglected?
- Is there evidence to suggest significant differences between nonlinear SSSI (the coupled building case) and nonlinear SSI (the uncoupled building case) analyses?

2. Theoretical modelling for SSSI

2.1 Non-dimensional equations of motion

The system shown in Figure 1 is described in terms of four generalised coordinates (or degrees of freedom) namely x_j to the translational DOFS and θ_j to the rotational DOFS, with $j \in [1,2]$. A known ground displacement field x_g is applied at both foundations, i.e. wave passage effects and spatially heterogeneous ground displacements are neglected in the present work. The effects of the horizontal stiffness of the foundations it is not considered in this paper. The kinetic energy T_E and potential energy U_E for this system are given by the following equations:

$$T_E = \frac{1}{2}\sum_{j=1}^{2}\left(m_{bj}\left(\dot{x}_j + \dot{x}_g - h_j\dot{\theta}_j\right)^2 + m_{sj}r_j^2\theta_j^2\right) \quad \textbf{(1)}$$

$$U_E = \sum_{j=1}^{2}\left(\frac{1}{2}k_{bj}x_{j1}^2 + \int M_j d\theta_j\right) + \frac{1}{2}\kappa(\theta_2 - \theta_1)^2 \quad \textbf{(2)}$$

where h_j are the heights of buildings, m_{bj} are building lumped masses (i.e. the generalised masses of the fundamental modes), m_{sj} are the foundation/soil masses underneath building 1 and 2, r_j are the soil/foundation mass's radii of gyration, $m_{sj}r_j^2$ are the foundation/soil mass polar second moments of area (moments of inertia). k_{bj} are the linear building lateral stiffnesses (i.e. the generalised stiffnesses of the fundamental modes), κ is the stiffness of inter-building soil rotational spring and b_j are the foundations width.

$M_j(\theta_j(t), y_j(t))$ are the nonlinear moments at the support springs, that are related to the rotational spring stiffnesses of soil beneath buildings 1 and 2. $y_j(t)$ are internal hysteretic rotation (history dependent of rotations θ_j) at time t, that controls the nonlinear response of the soil. In this paper, we assume that the stiffness associated to the inter-building interaction κ through the soil it is considered linear. The rationale behind this is that the soil strains between buildings are likely to be far smaller than directly under the footing. Hence, the system's nonlinear behaviour is presumed encapsulated by a nonlinear Bouc-Wen spring model for the footing alone and a linear interaction spring model of type [17-18]. It is also worth noting that an analytical formulation for a linear interaction spring has only just been published [46], while there exists no nonlinear interaction spring model in the literature.

With the aim of non-dimensionalising the problem, this nonlinear moment/rotation function $M_j(\theta_j(t), y_j(t))$ shall be replaced by the following term, where $q_j\left(\theta_j(t), y_j(t)\right)$ is a non-dimensional nonlinear moment/rotation functions of the foundation/soil and k_{sj} are the initial linear rotational stiffnesses of soil beneath buildings when $\theta_j = 0$ at $t = 0$.

$$M_j = k_{sj}q_j \quad \textbf{(3)}$$

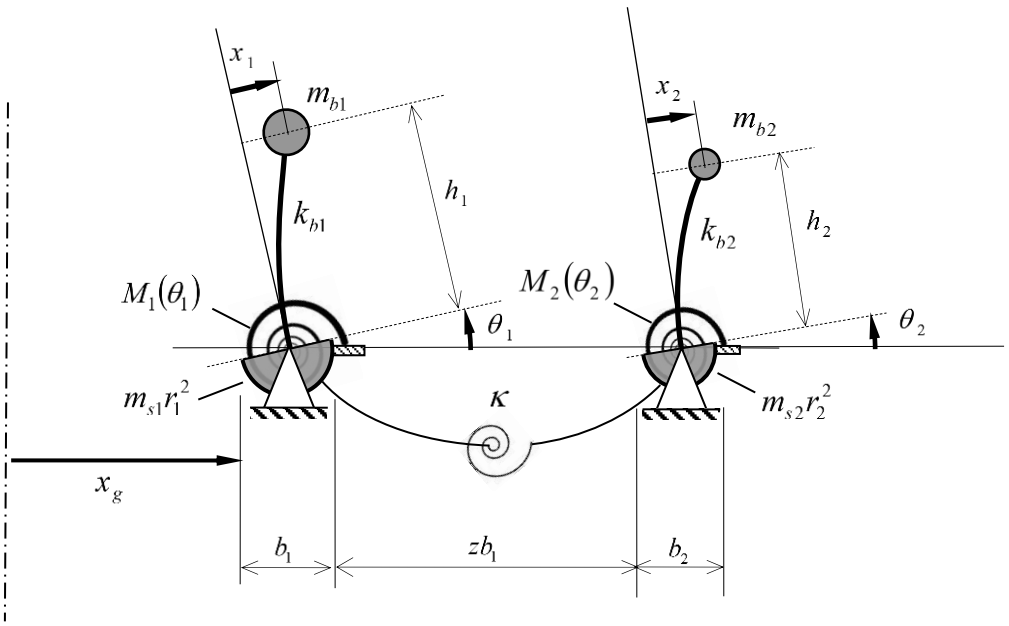

Figure 1. Two building system.

We can introduce the following non-dimensional parameter groups,

$$\eta_j = \frac{h_j}{r_j},\ \ \alpha_j = \frac{m_{bj}}{m_{sj}},\ \ \beta = \frac{r_1}{r_2},\ \ \lambda = \frac{m_{b2}r_2^2}{m_{b1}r_1^2},\ \ \varpi = \frac{\kappa}{m_{b1}r_1^2} \tag{4}$$

and the frequency parameters,

$$\omega_1^2 = \frac{k_{b1}}{m_{b1}},\ \ \omega_2^2 = \frac{k_{s1}}{m_{s1}r_1^2},\ \ \omega_3^2 = \frac{k_{b2}}{m_{b2}},\ \ \omega_4^2 = \frac{k_{s2}}{m_{s2}r_2^2} \tag{5}$$

and non-dimensional frequency ratios,

$$\Omega_2 = \frac{\omega_2}{\omega_1},\ \ \Omega_3 = \frac{\omega_3}{\omega_1},\ \ \Omega_4 = \frac{\omega_4}{\omega_1},\ \ \Omega_0 = \frac{\varpi}{\omega_1} \tag{6}$$

Finally, we introduce the following change of variables that completes the full non-dimensionalisation of the problem, where ω_1 is the modal circular frequency on a fixed base (i.e. with no foundation/soil rotation) of the building 1, u_j are non-dimensional relative displacement of buildings to ground and u_g is the non-dimensional horizontal ground displacement (absolute).

$$x_j = r_j u_j,\ \ x_g = r_1 u_g,\ \ \tau = \omega_1 t \tag{7}$$

Therefore, after some calculus, the Euler-Lagrange equations of motion can be stated thus,

$$\mathbf{M\ddot{u}} + \mathbf{C\dot{u}} + \mathbf{Ku} + \mathbf{q}(\theta, y) = \mathbf{f}\ddot{u}_g \tag{8}$$

where Newtonian dots above now indicated derivatives with respect to scaled time τ, i.e. $(\dot{\bullet}) = \partial\bullet/\partial\tau$ and $(\ddot{\bullet}) = \partial^2\bullet/\partial\tau^2$. The matrices and vectors for the above equation are stated as follows,

$$\mathbf{M} = \begin{bmatrix} 1 & -\eta_1 & 0 & 0 \\ -\eta_1 & \alpha_1 + \eta_1^2 & 0 & 0 \\ 0 & 0 & \lambda & -\eta_2\lambda \\ 0 & 0 & -\eta_2\lambda & \lambda(\alpha_2 + \eta_2^2) \end{bmatrix},\ \mathbf{K} = \begin{bmatrix} 1 & 0 & 0 & 0 \\ 0 & \Omega_0^2 & 0 & -\Omega_0^2 \\ 0 & 0 & \lambda\Omega_3^2 & 0 \\ 0 & -\Omega_0^2 & 0 & \Omega_0^2 \end{bmatrix},\ \mathbf{u} = \begin{bmatrix} u_1 \\ \theta_1 \\ u_2 \\ \theta_2 \end{bmatrix},\ \mathbf{f} = \begin{bmatrix} -1 \\ \eta_1 \\ -\lambda\beta \\ \eta_2\lambda\beta \end{bmatrix} \tag{9}$$

The system's linear viscous damping matrix $\mathbf{C}$ defined in equation (8) assume that each natural mode $n \in [1,4]$ is damped at $\xi_n = 0.05$ of critical damping, $\boldsymbol{\phi}_n$ is the modal vector of the mode n, ω_n are the natural frequencies of the systems. These ω_n were calculated considering the completely elastic system described in Alexander et al. [17], thus the Caughey damping matrix $\mathbf{C}$ can be calculated as [38]:

$$\mathbf{C} = \mathbf{M}\left(\sum_{n=1}^{4} \frac{2\xi_n\omega_n}{\boldsymbol{\phi}_n^T\mathbf{M}\boldsymbol{\phi}_n}\boldsymbol{\phi}_n\boldsymbol{\phi}_n^T\right)\mathbf{M} \tag{10}$$

This viscous model includes the linear contribution to damping. Additional nonlinear contributions to damping of the soil are provided by the Bouc-Wen hysteretic model. The nonlinearity in the equation (8) is contained in vector $\mathbf{q}(\theta, y)$ that is defined as:

$$\mathbf{q}(\theta_j, y_j) = \begin{bmatrix} 0 \\ B_1\Omega_2\theta_1 \\ 0 \\ B_2\Omega_4\theta_2 \end{bmatrix} + \begin{bmatrix} 0 \\ (1 - B_1)\Omega_2 y_1 \\ 0 \\ (1 - B_2)\Omega_4 y_2 \end{bmatrix} \tag{11}$$

$$k_{sj} = \frac{1}{2}\frac{G_s b_j^3}{1 - \mu} \tag{12}$$

where y_j is the internal degrees of freedoms that controls the nonlinear response of soil, $0 \leq \mathrm{B}_j \leq 1$ is the ratio of linear to nonlinear response (defined below according to the Bouc-Wen model). Rotational stiffnesses k_{sj} are obtained by using an empirical formula (deducted by Gorbunov-Possadov et al. [23]) for the rotational stiffness coefficient of soil beneath buildings 1 and 2, G_s is the initial tangent shear modulus of the soil and μ is the Poisson's ratio of the soil.

Note that both linear and nonlinear support rotational moment/rotation relationship is contained in vector $\mathbf{q}(\theta, y)$. Note if $\mathrm{B}_j = 1$ then this system reduces to a linear system described in references [17,18].

2.2 Bouc-Wen model for nonlinear soil rotational springs

The Bouc-Wen hysteretic model, in all its various forms [24-29], is widely used in the literature for systems that exhibit inelastic behaviour under severe cyclic loads. The attractiveness of this approach is that it employs a first order differential equation in terms of an 'internal hysteretic' variable y_j to describe, qualitatively the phenomenological nonlinear hysteretic behaviour. The model reproduces the nonlinear hysteretic behaviour of a variety of soils and it is capable of representing complex patterns such as stiffness and strength degradation with cycling loading. This approach contrasts with the "rule-based" hysteretic models of Takeda [30], Ramberg-Osgood [31] and others that require more complex coding than a Bouc-Wen model.

The non-dimensional nonlinear moment/rotation function, of *j*th building foundation, is described by the following Bouc-Wen nonlinear differential equation;

$$\dot{y}_j = \frac{1}{\gamma_y} \frac{D_j \dot{\theta}_j - v(E)\left(\varsigma_j |\dot{\theta}_j| |y_j|^{n_j} \mathrm{sgn}(y_j) + \psi_j \dot{\theta}_j |y_j|^{n_j}\right)}{\eta(E)} \tag{13}$$

In the above expression, γ_y is the strain at the initiation of nonlinear behaviour in the soil that has been defined by various studies in the literature, Ishibashi and Zhang [32], Tatsuoka et al. [33], Hardin and Drnevich [44] among others. In this paper we adopt a value of $\gamma_y = 10^{-4}$ for sand, $[D_j, \varsigma_j, \psi_j, n_j]$ represent the dimensionless Bouc-Wen parameters that define the shape of the hysteretic stress-strain loops, B_j is the ratio of linear to nonlinear response, δ_v is the strength degradation parameter and δ_η is the stiffness degradation parameter. $v(E)$ and $\eta(E)$ characterize the degradation shape functions, that are dependent to the dissipated hysteretic energy $E(\tau)$ from initial time $\tau = 0$ to the present time τ.

$$E(\tau) = \int_0^\tau y \dot{\theta} d\tau\,, \;\; v(E) = 1 + \delta_v E(\tau), \;\; \eta(E) = 1 + \delta_\eta E(\tau) \tag{14}$$

In this paper, we use the values for Bouc-Wen parameters proposed by Gerolymos and Gazetas [34-35] and Drosos et. al [36], (see table 1) that give a reasonable shape for soil spring and damping stress-strain curves for all examined soil profiles. These values provide a good representation of the complex nonlinear characteristics of the cyclic behaviour of the soil element.

Table 1. Bouc-Wen nonlinear soil model parameters

Soil	γ_y	D_j	B_j	ς_j	ψ_j	δ_v	δ_η	n_j
Sand	10^{-4}	1	0.02	0.5	0.5	0.01	0.01	0.6

2.3 Reduced parametric form

Equation (8) is expressed in terms of ten linear system parameters η_1, η_2, α_1, α_2, λ, Ω_0, Ω_2, Ω_3, Ω_4 and ω_1 plus our eight constants that define the Bouc-Wen model. Additionally, the ground excitation has its own statistical descriptors which can be viewed as further system parameters. Therefore, we have an extremely large system parameter space to explore for a comprehensive parametric study. To reduce this number, we follow the procedure described in [17] where the scope of our analysis is limited by assuming that:

(i) *the same soil profile exists under both buildings, this means* $k_{s1} = k_{s2}$
(ii) *both buildings have a similar square plan area of* b^2, *where* $r_1 = r_2 = 0.33b$
(iii) *both buildings have the same average density,* ρ_b
(iv) *the buildings can be of different heights,* h_j
(v) *the buildings are spaced at some arbitrary distance from each other,* zb_1.
(vi) *the mean system response to a set of ground motion time-series is estimated by using a single spectrally match ground motion time-series.*

Newmark and Rosenblueth [37] proposed that the dynamic mass of soil beneath buildings is equal to $m_s = 0.35b^3\rho_s$, the mass of the buildings can be calculated as $m_{bj} = \rho_b h_j b^2$, where ρ_s and ρ_b are the densities of soil and building respectively. Parameters η_1, η_2, α_1, α_2 are contracted into two geometric parameters *Height ratio* ε and *Aspect ratio* s, where the proportionality constant c_1 is defined in table 2.

$$\varepsilon = \frac{h_2}{h_1},\ \ s = \frac{h_1}{b},\ \ \eta_1 = 3s,\ \ \eta_2 = 3\varepsilon s,\ \ \alpha_1 = \frac{c_1}{s},\ \ \alpha_2 = \frac{c_1}{\varepsilon s},\ \ c_1 = 0.35\frac{\rho_s}{\rho_b} \tag{15}$$

The frequency ratio parameters Ω_0, Ω_2, Ω_3 and Ω_4, the ratio of foundation radii of gyration β and the ratio of foundation mass polar moments of inertia λ are contracted and re-expressed in terms of:

$$\Omega_0^2 = c_1 c_2 q_2 q_\kappa s\overline{V}_s^2,\ \ \Omega_2^2 = \Omega_4^2 = c_2 q_2 s^2\overline{V}_s^2,\ \ \Omega_3 = \frac{1}{\varepsilon},\ \ \lambda = \varepsilon,\ \ \beta = 1 \tag{16}$$

$$V_s^2 = \frac{G_s}{\rho_s},\ \ \overline{V}_s = \frac{V_s}{1000},\ \ \omega_1 \approx \frac{200}{h_1},\ \ \omega_3 \approx \frac{200}{h_2} \tag{17}$$

Where the natural period T of a structure (on a rock foundation) is equal to the empirical relationship $T = n/10\ [s]$ [40], n is the number of storeys of the buildings (3.2m average storey height), V_s is shear wave velocity of the soil in [m/s]. $\bar{V}_s$ is the normalised non-dimensional shear wave velocity (to a reference of 1000 m/s) and soil constant c_2; both are defined in table 2. The interaction spring κ is modelled using an inverse cube relationship between κ and k_2[17].

$$\kappa = q_k(z)q_2(z)k_s,\ \ q_k(z) = \frac{-0.25}{(1+z)^3},\ \ q_2(z) = 1 + \frac{0.5}{(1+z)^3} \tag{18}$$

Table 2. Linear elastic stiffness parameters for soil classes

Soil Class (sand)	$\rho_s[kg/m^3]$	μ []	c_1 []	c_2 []	V_s $[m/s]$
Dense	2000	0.35	1.17	503.5	325
Medium	1600	0.30	0.93	468	250
Loose	1300	0.30	0.76	468	156

Thus, we can re-express system matrices (9) in terms of 3 geometric non-dimensional parameters (i) aspect ratio $s = h_1/b$ (for building 1), (ii) the height ratio $\varepsilon = h_2/h_1$ (building 2 to 1), (iii) the normalised inter-building distance ratio z (the ratio of distance between buildings to building width), iv) one soil class that is defined using c_1, c_2, $\bar{V}_s$, ρ_s and μ (see table 2).

$$\mathbf{M} = \begin{bmatrix} 1 & -3s & 0 & 0 \\ -3s & c_1 s^{-1} + 9s^2 & 0 & 0 \\ 0 & 0 & \varepsilon & -3\varepsilon^2 s \\ 0 & 0 & -3\varepsilon^2 s & c_1 s^{-1} + 9\varepsilon^3 s^2 \end{bmatrix}, \quad \mathbf{K} = \begin{bmatrix} 1 & 0 & 0 & 0 \\ 0 & \Omega_0^2 & 0 & -\Omega_0^2 \\ 0 & 0 & \varepsilon^{-1} & 0 \\ 0 & -\Omega_0^2 & 0 & \Omega_0^2 \end{bmatrix}, \quad \mathbf{f} = \begin{bmatrix} -1 \\ 3s \\ -\varepsilon \\ 3\varepsilon^2 s \end{bmatrix} \tag{19}$$

The nonlinear vector $\mathbf{q}(\theta, y)$ in its nondimensional form can be evaluate as:

$$\mathbf{q}(\theta, y) = B_1 c_1 c_2 q_2 s \overline{V}_s^2 \begin{bmatrix} 0 & 0 & 0 & 0 \\ 0 & 1 & 0 & 0 \\ 0 & 0 & 0 & 0 \\ 0 & 0 & 0 & 1 \end{bmatrix} \begin{bmatrix} u_1 \\ \theta_1 \\ u_2 \\ \theta_2 \end{bmatrix} + (1 - B_1) c_1 c_2 q_2 s \overline{V}_s^2 \begin{bmatrix} 0 & 0 & 0 & 0 \\ 0 & 1 & 0 & 0 \\ 0 & 0 & 0 & 0 \\ 0 & 0 & 0 & 1 \end{bmatrix} \begin{bmatrix} u_1 \\ y_1 \\ u_2 \\ y_2 \end{bmatrix} \tag{20}$$

2.4 Defining system performance measures

As a measure of change in the response between the coupled (SSSI) and uncoupled (SSI) systems, in this study we will use the following performance measures.

$$U_j = u_j - 3\frac{h_j}{b}\theta_j, \quad A_j = \ddot{u}_j + \ddot{u}_g - 3\frac{h_j}{b}\ddot{\theta}_j \tag{21}$$

Where U_j and A_j are the relative (sway + rotational) displacement and total (sway + ground + rotational) accelerations of buildings "j" in non-dimensional form. Additionally, we use the percentage change χ in mean squared (the total power) response caused by building interactions, when moving from uncoupled (SSI) to coupled cases (SSSI).

$$\chi_{jj} = 100\frac{\left[E_s(q_j)\right]_{SSSI} - \left[E_s(q_j)\right]_{SSI}}{\left[E_s(q_j)\right]_{SSI}} \tag{22}$$

Where the total power spectral density E_s (which is based on all data points) is defined as follows using Parseval's theorem,

$$E_s(q_j) = \int_{-\infty}^{\infty} \left|q_j(\tau)\right|^2 d\tau = \frac{1}{2\pi}\int_{-\infty}^{\infty} \left|Q_j(\omega)\right|^2 d\omega \tag{23}$$

By using the Fourier transform of $q_j(\tau)$ we can obtain the power spectral density function $Q_j(\omega)$. Function $q_j(\tau)$ in the above expression is simply either displacement $U_j(\tau)$ and or acceleration $A_j(\tau)$. Using equation (23) delivers a statistical estimation of magnitude that is more robust than employing a single peak of the function. To obtain the uncoupled system response (SSI) case we set the rotational interaction spring κ equal to zero, which is equivalent to an increase inter-building distance z to a very large value.

3. Analyses

As a parametric study, the response of the system depends on the aspect ratio $s = h_1/b$, height ratio $\varepsilon = h_2/h_1$, soil type and inter-building distance z. The Bouc-Wen parameters are assumed constants and defined above in table 1.

We will first explore the differences in the seismic response of linear/nonlinear SSSI and linear/nonlinear SSI problems for a test case of loose soil and closely spaced buildings. Alexander et al. [17] suggested that the largest percentage change (SSI) to (SSSI) occurs for loose soil and closely spaced buildings, therefore, we adopt loose soil and inter-building case $z = 0.1$ as a test case. Secondly, we extend this analysis to consider the effects of height ratio and aspect ratio. Finally, we explore the effect of soil type and inter-building spacing.

3.1 Ground motion selection

In order to determine the effect of SSSI on the system equation (8), it is analysed considering a horizontal component ground motion matched with a specific target response spectra. In this way, we significantly reduce the number of nonlinear time-history analyses performed while approximating the mean system response to a set of ground motion time-series that are compatible with the EC8 elastic spectrum. In future work, a complete set of different ground motion records will be considered. The original ground motion time series is from the event in Imperial Valley California, USA, in 1979 with a magnitude of M_w=6.5 and a peak ground acceleration (PGA) equal to a_{gr} = 0.37g. This ground motion was obtained from the Pacific Earthquake Engineering Research (PEER) Center Database [41], recorded on weak soils with a shear wave velocity equal to 175 m/s.

The target horizontal elastic response spectrum $S_a(T)$ chosen in this study was the response spectra defined in Eurocode 8, Part 1 [42], considering a design ground acceleration equal to a_g = 0.6g, ground type equal to "D" (i.e. deposit of loose to medium cohesionless soil with a shear wave velocity V_s < 180 m/s). A viscous damping ratio of the structure ξ = 5% (damping correction factor equal to η_s=1) and the magnitude of the seismic corresponding to type 1 (the earthquake had a surface-wave magnitude M_s > 5.5.). The design ground acceleration represents a high seismic zone, with a magnitude of M_w=7.5 and an epicentre distance of 8km [56]. This high seismic excitation produce significant nonlinear response in the soil beneath the buildings.

The Reweighted Volterra Series Algorithm (RVSA) proposed by Alexander et al. [43] is employed. This spectral matching process is stable and robust because it converges to any reasonable response spectrum for any suitable seed time-series and keeps the non-stationary characteristics (e.g. timing of the main pulse, the variation of frequency content with time and general envelope) of the original record. Note that the EC8 spectrum is extended from 4 to 10s. This extension to the target spectrum enables the RVSA spectral matching process to significantly reduce the low-frequency content of the spectrally matched time-series. The RVSA re-express the ground motion time series as a discrete Volterra series, then using a complete multinomial mixing of the first-order kernel functions the higher-order Volterra kernels are estimated. Finally, the optimal weighting of each term within each Volterra kernel is obtained using Levenberg-Marquardt approach. The matched, target and original response spectra are shown in Figure 2(a). Figure 2(b) shows the original (seed) and matched time-series. This demonstrates that the match time-series maintains the overall envelope and locations of pulses of the original time-series while matching much more closely a target spectrum.

3.2 Comparison between linear and nonlinear soil

We investigate the difference in the dynamic response between the linear and nonlinear cases considering the dynamic coupling of adjacent buildings. For this, we examine the case when two buildings are very close to each other. i.e. at a spacing distance equal to $z = 0.1$ of building's base width b, fixed base frequency of the

building 1 equal to $\omega_1/2\pi = 4.0$Hz, aspect ratio $s = 1.5$ and height ratio $\varepsilon = 1.5$ (i.e. the second building is 50% taller than the first building and building one has a height to width ratio of 1.5).

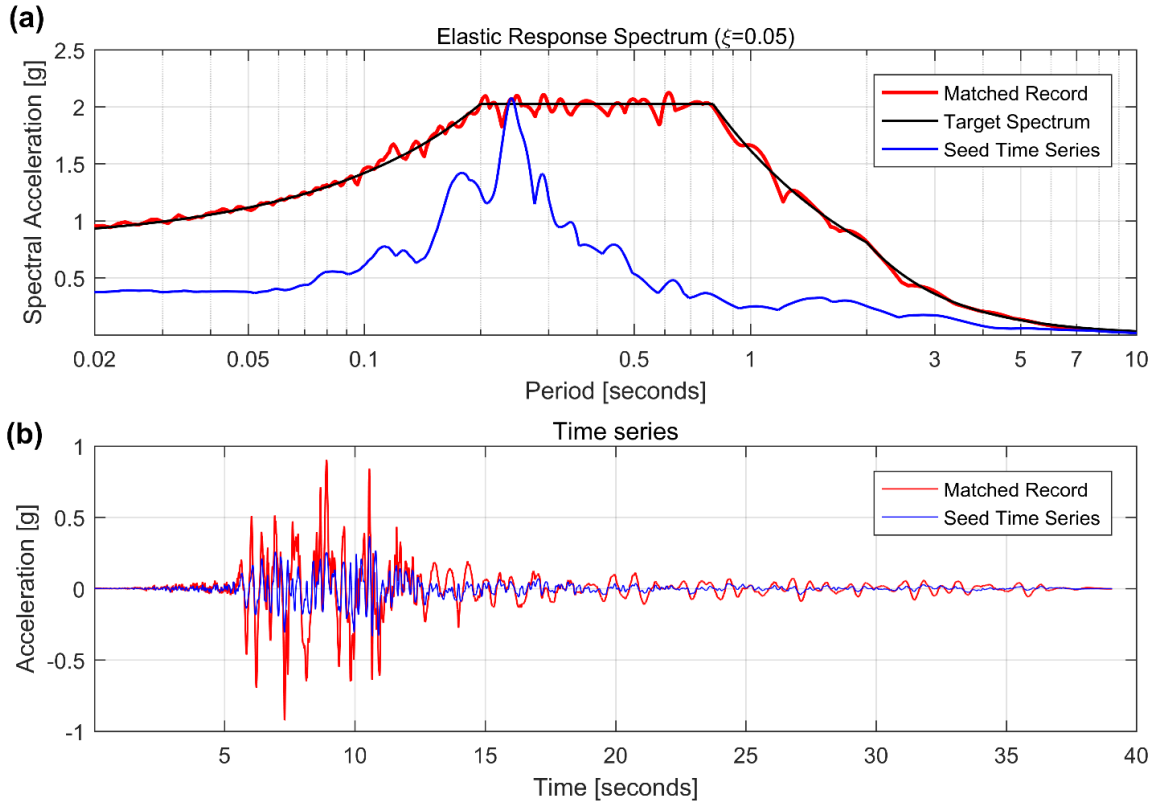

Figure 2. (a) Matched, target and seed response spectra (ξ = 0.05) (b) Matched and seed (original) time-series.

Figure 3(a) shows the linear (blue line) and nonlinear (red line) response of the buildings 1 and 2 considering the coupled effect in terms of the displacement U_j. Comparing the responses we observe that the maximum displacement of the buildings increases when nonlinear behaviour in the soil is included. Likewise, in Figure 3(b) we can observe that the maximum displacement of the buildings 1 and 2, for uncoupled (SSI) case, increase when nonlinear behaviour in the soil (red line) is assumed. This difference in behaviour is expected since the structural system becomes softer at the point where soil strain exceeds $\gamma_y = 10^{-4}$ and therefore the rotational spring stiffness decreases in each subsequent large amplitude cycle.

Figure 3(c) shows the power spectral density for the displacements considering four cases: (i) coupled (linear SSSI), (ii) uncoupled (linear SSI) elastic response (iii) coupled (nonlinear SSSI) and (iv) uncoupled (nonlinear SSI) response. Comparing the linear and nonlinear responses we observe that building 1 is significantly affected. Building 1's response power increases by $\chi_{11} = 323[\%]$, for nonlinear SSSI case, in the presence of the taller building 2. Conversely, its response power only increases by $\chi_{11} = 34.6[\%]$, for the linear SSSI case. In an equivalent way for the building 2 has a larger reduction in response power $\chi_{22} = -57.7[\%]$ (nonlinear SSSI), than in the linear case $\chi_{22} = -20.6[\%]$ (linear SSSI). Thus, we observe that both adverse and beneficial responses can appear greater in the nonlinear SSSI cases.

Figure 3(a) displays the displacement time-series, for the nonlinear SSSI case, and it does not return to zero at the end of the seismic excitation. This is highlighted by the power spectra in figure 3(c) where the DC term (the zero frequency component) is 75dB/Hz, 12dB/Hz and 1.5dB/Hz for the coupled (nonlinear SSSI), uncoupled (nonlinear SSI) and uncoupled (linear SSI) cases respectively in the building 1. This DC term is proportional to the mean of the time series [45]. This suggests the nonlinear SSSI analyses may exhibit seriously

greater asymmetric oscillations than nonlinear SSI analyses. Therefore, there is the significantly greater probability of the buildings coming to rest leaning at some angle if SSSI is performed.

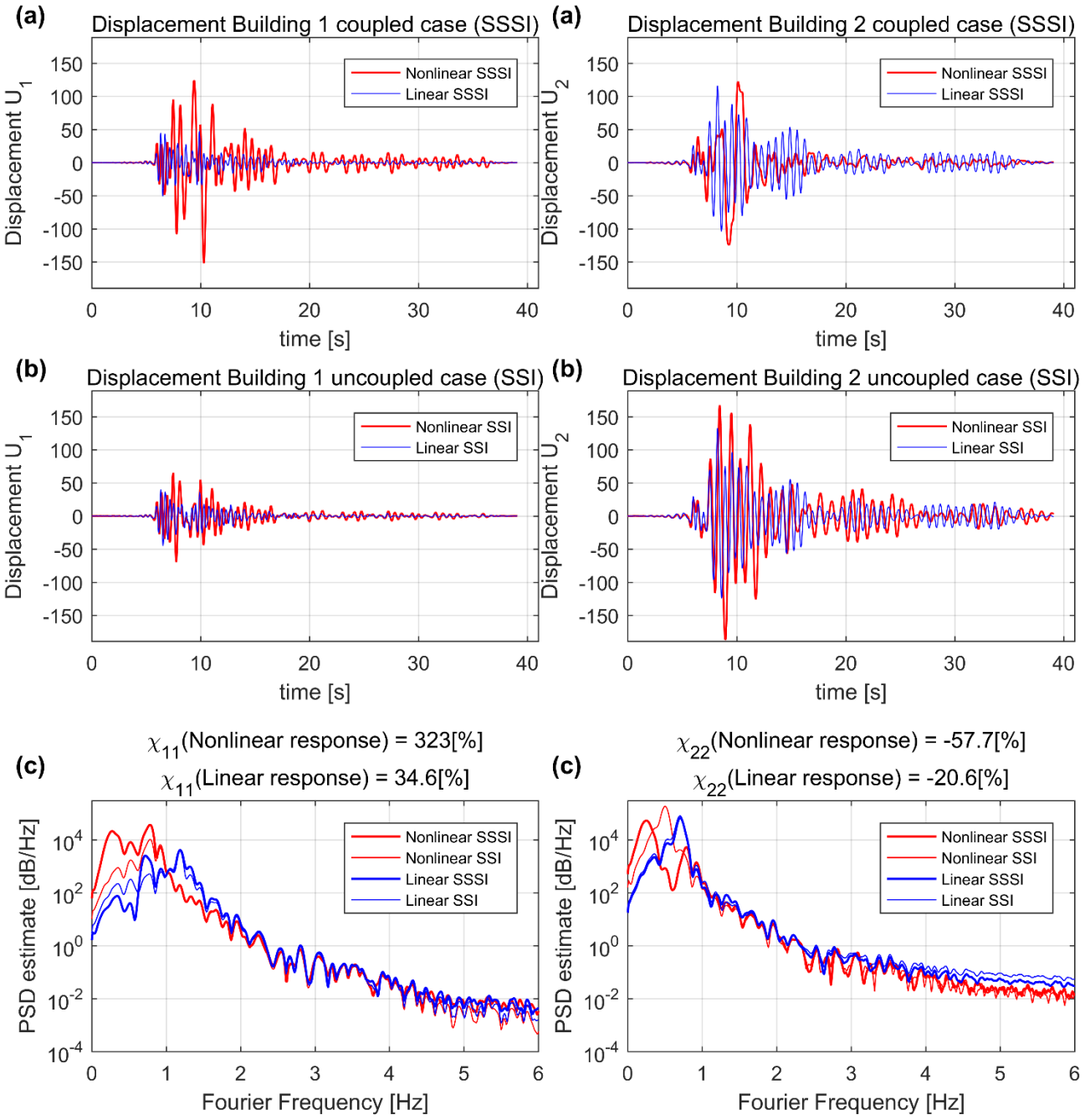

Figure 3. (a) Displacement response coupled case (b) Displacement response uncoupled case (c) power spectra density – Response on loose soil for parameter set (ε=1.5, s=1.5, z=0.1).

Figure 4(a) shows the linear/nonlinear SSSI total acceleration A_j responses of the buildings 1 and 2. Figure 4(b) displays the acceleration of building 1 and 2 for the uncoupled (SSI) case. We can see from these four graphs that, in general, the total acceleration of the buildings reduces with the introduction of nonlinear behaviour which is expected. Figure 4(c) shows the corresponding power spectral density for the total acceleration and the percentage change in total response power $\ddot{\chi}_{11}[\%]$, considering the four cases. For both cases respectively, linear and nonlinear, it can be observed that building 1's total response power increases by about 27.8% and 95.4% and building 2's reduces by 14.8[%] and 67.9[%]. It is noted that unlike displacement the DC terms are close to zero (0.15dB/Hz) suggesting that the mean total accelerations are negligible. In

addition, the Figure 4(c) illustrates the drop in the peak frequency system response between the linear and nonlinear case. This is a typical behaviour of softening nonlinear systems.

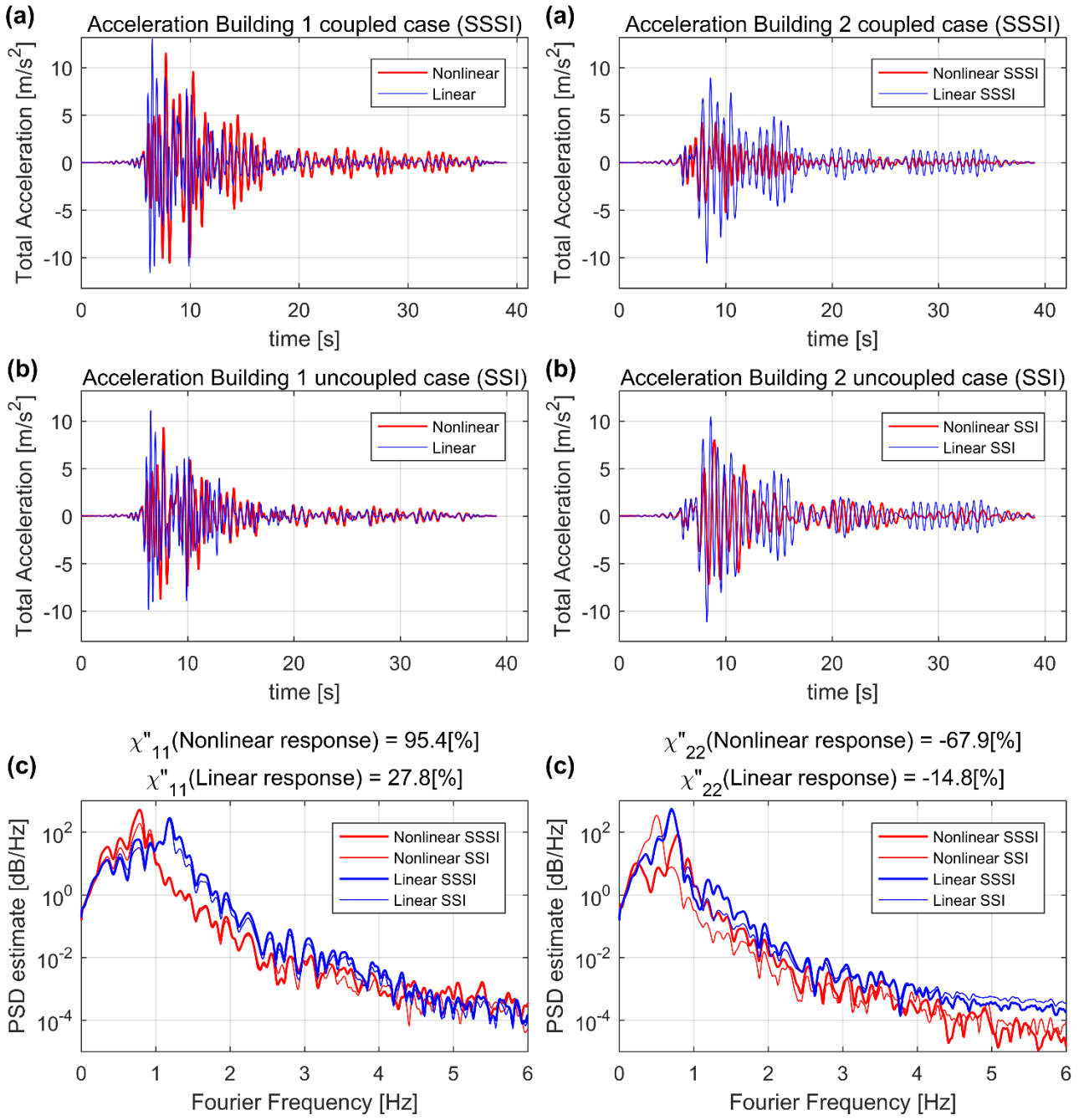

Figure 4. (a) Total acceleration response coupled case (b) Total acceleration response uncoupled case (c) power spectra density – Response on loose soil for parameter set (ε=1.5, s=1.5, z=0.1).

Figure 5 depicts the hysteresis cycles in the soil/foundation of the buildings 1 and 2 under the seismic action, computed by the Bouc-Wen model. The moment-rotation loops are consistent with the shear modulus and damping curves of the literature and correspond to the hysteretic soil behaviour experimentally observed [34].

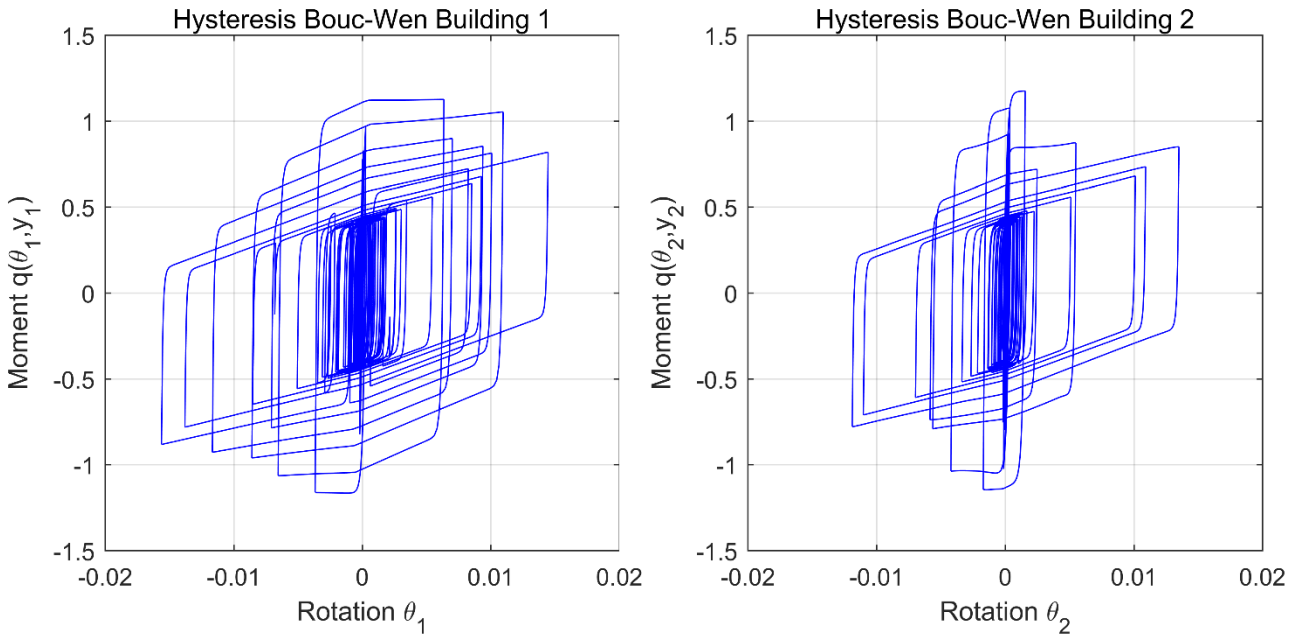

Figure 5. Hysteresis loops for the soil beneath buildings 1 and 2 (nonlinear SSSI) – Response on loose soil for parameter set (ε=1.5, s=1.5, z=0.1).

3.3 Change in power considering nonlinear soil with variation in aspect ratio s, height ratio ε and soil type.

We now can take a look at the variation of change of power $\chi_{11}(s,\varepsilon)$ for the case with linear behaviour of the soil, i.e. be setting Bouc-Wen parameter $B_j = 1$. Figure 6 displays the contour plots of $\chi_{11}(s,\varepsilon)$ for the displacement U_1 and acceleration A_1 of building 1. The critical zones in the figure are red, i.e. where the buildings 1's total response power is amplified by the presence of building 2 and blue when the response is reduced. The worst possible building parametric configuration lies around $\chi_{11}(0.25,1.3) = 65\%$ and $\ddot{\chi}_{11}(2.0,1.2) = 85\%$ for the displacement and acceleration respectively.

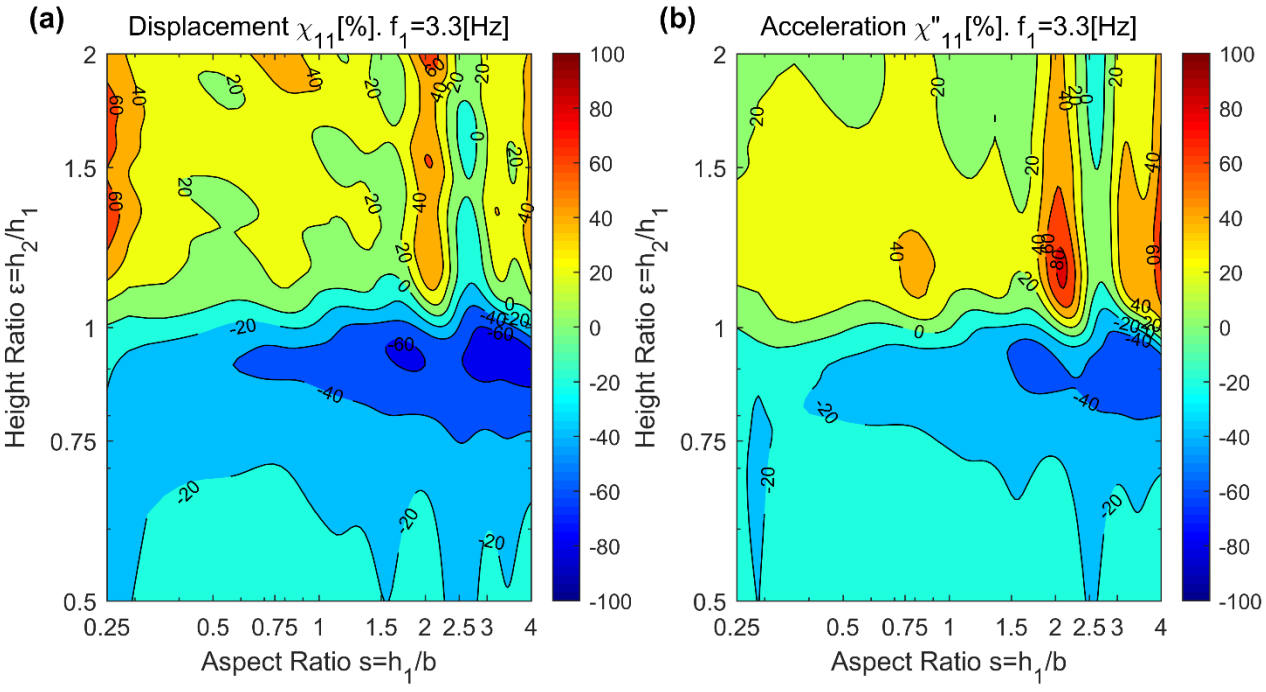

Figure 6. (a) Change in displacement power χ_{11} with the aspect and height ratio (b) Change in acceleration power $\ddot{\chi}_{11}$ with the aspect and height ratio – Linear response on loose soil and z=0.1.

As previously stated, the change of power $\chi_{11}(s,\varepsilon)$ mainly depends on the aspect ratio s, height ratio ε, soil class and inter-building distance z. This is similar to the linear case [17-18]. Contour plots in Figure 7(a) show the variation of change of power $\chi_{11}(s,\varepsilon)$ with height and aspect ratio for the displacement of the building 1, U_1. With the aim of making the figure more readable, the change in the colour contour is shown up to a value of 100% and for larger values only the contour line is marked. We consider loose soil and inter-building case equal to $z = 0.1$. In general, it can be observed that the power of earthquake passes from the taller building to the smaller building, increases dramatically when the height ratio is greater than 1.5, reaching values above 400% amplification. As in figures 3(c), this is due to significant low-frequency content. Large asymmetrical oscillations of the building increase the probability of a large residual rotation of building 1 after the earthquake shaking has finished, as shown in the contour plots of Figure 8 with a maximum value of residual rotation are 0.73 degree and 0.26 degree for the nonlinear SSSI Figure 8(a) and nonlinear SSI Figure 8(b) respectively.

Comparing figure 7(a) and figure 6(a) suggests that including nonlinearity smooths out the parametric variation in total power responses due to the limiting value of soil-spring capacity assumed in the Bouc-Wen model. For both figures, a 100x100 grid of parametric values for the height and aspect ratio.

Thus, the interaction effect between the buildings increases when the nonlinear behaviour in the soil is considered. This highlights the importance to consider the dynamic coupling (nonlinear SSSI) of adjacent buildings when the structures are very close especially when extreme seismic loads produce predominantly nonlinear behaviour in the system. On the other hand, the reduction of the response is limited to a maximum value of $\chi_{11}(0.75,0.75) = -45[\%]$ for a height ratio $\varepsilon < 1.0$. Unlike to the linear SSSI shown in Figure 6, this reduction does not apply for the entire range of aspect ratio.

Figure 7(b) displays the change of power $\ddot{\chi}_{11}(s,\varepsilon)$ for the total acceleration of the building 1 A_1, where unlike the previous case the maximum amplification is limited to certain values of height and aspect ratio. In this case, the worst possible configuration is when the second building is 75[%] taller than the first and the foundation width of the buildings is 1.1 times the height of the building 1, $\ddot{\chi}_{11}(0.9,1.75) = 110[\%]$.

Each contour plot, presented in this paper, required approximately 150 hours runtime on the BlueCrystal, the High-Performance Computing (HPC) machine belonging to the Advance computing research centre at the University of Bristol.

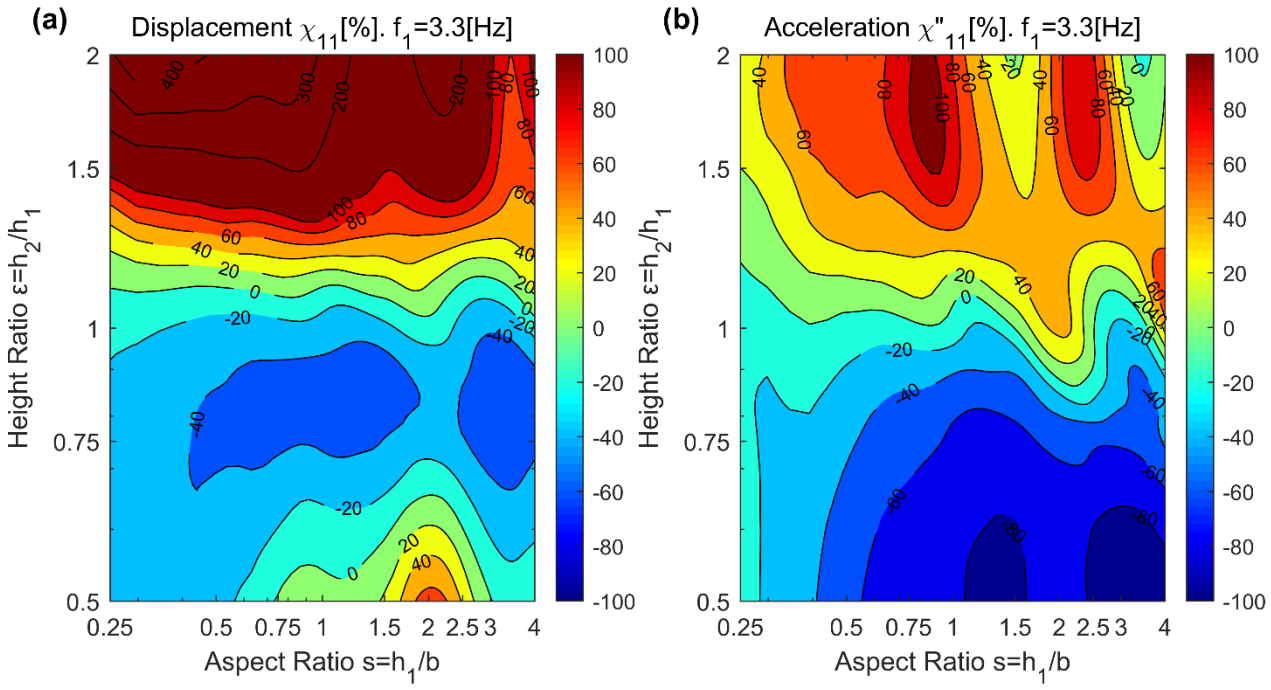

Figure 7. (a) Change in displacement power χ_{11} with the aspect and height ratio (b) Change in acceleration power $\ddot{\chi}_{11}$ with the aspect and height ratio – Nonlinear response in loose soil and z=0.1.

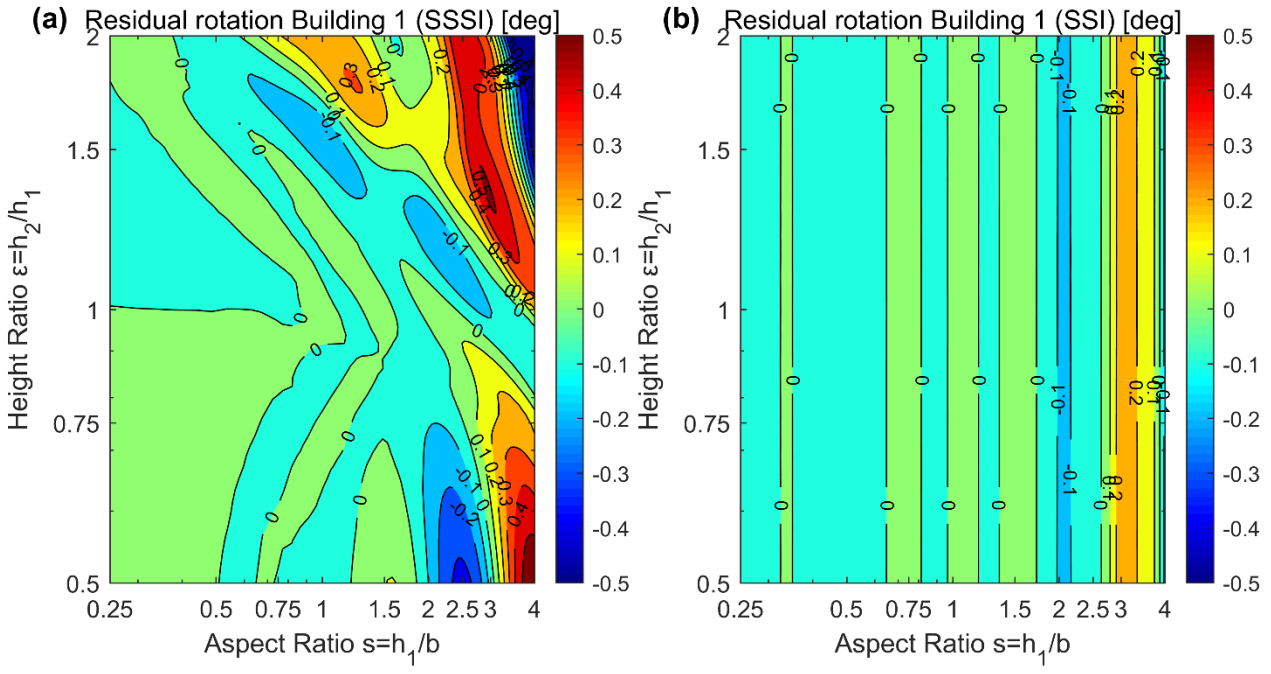

Figure 8. (a) Residual rotation with the aspect and height ratio (nonlinear SSSI) (b) Residual rotation with the aspect and height ratio (nonlinear SSI) – Response on loose soil and z=0.1.

Figure 9 displays the previous analysis for the case of dense sand and a nonlinear analysis case. In this case, the amplification/reduction in the change of power are more limited, $\chi_{11}(2.0,2.0) = 250\%$ and $\ddot{\chi}_{11}(3.0,1.8) = 45\%$ to the displacement and acceleration respectively, suggesting that the worst seismic interaction conditions occur on loose soil.

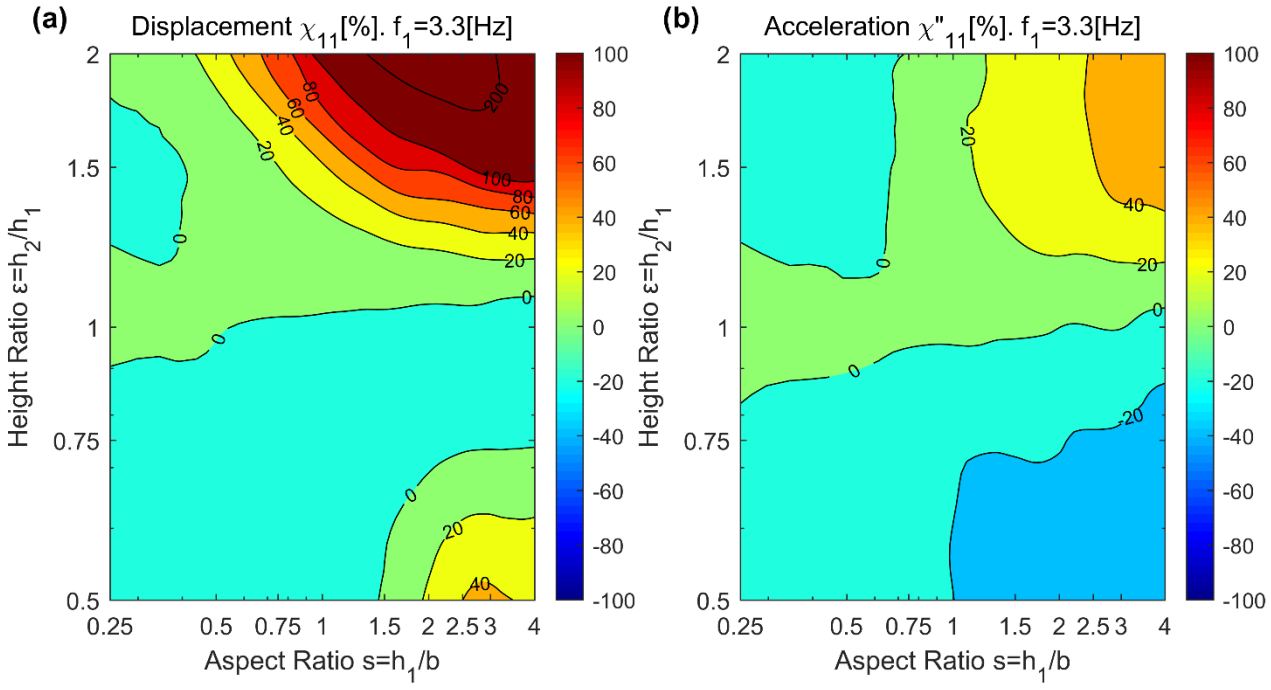

Figure 9. (a) Change in displacement power χ_{11} with the aspect and height ratio (b) Change in acceleration power $\ddot{\chi}_{11}$ with the aspect and height ratio – Nonlinear response on dense soil and z=0.1.

3.4 Change in power considering nonlinear soil due to variation in inter/building spacing z

Figure 10(a) shows the variation of power $\chi_{11}(s, \varepsilon, z)$ for the displacement with height ratio $\varepsilon = h_2/h_1$ and inter-building spacing z. The aspect ratio was set equal to $s = 3.0$. As expected the effects of SSSI decreases when increasing the inter-building spacing. At a distance between foundations equal to $2b$, the SSSI is practically negligible $\chi_{11}(3.0, \varepsilon, 2.0) = 4.5\%$. This result happens for any value of aspect ratio s. As discussed above, there is a sharp increase in the change in power for height ratio greater than 1.5, therefore as not to distort the Figure 11, the colour contour is only shown up to 100%.

Figure 10(b) repeats the previous analysis for the change of power $\ddot{\chi}_{11}(s, \varepsilon, z)$ for the acceleration and similarly, the interaction effect drops more sharply with increasing the inter-building spacing to a value of $\ddot{\chi}_{11}(3.0, \varepsilon, 2.0) = 3.8\%$.

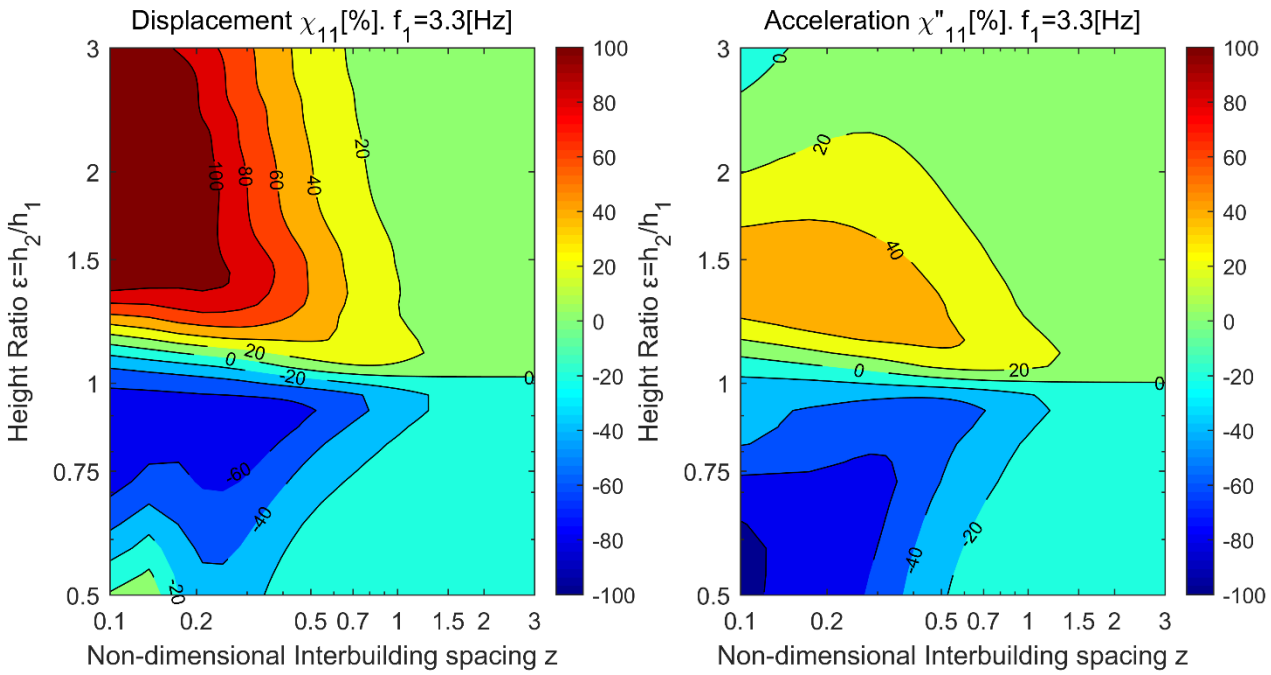

Figure 10. (a) Change in displacement power χ_{11} with the height ratio and inter-building spacing z (b) Change in acceleration power $\ddot{\chi}_{11}$ with the height ratio and inter-building spacing z – Nonlinear response on loose soil and aspect ratio s=3.0.

4. Conclusion

In this paper, we present a theoretical formulation for the 2-D SSSI between two buildings that are coupled through the soil and it is considered a nonlinear phenomenological Bouc-Wen model for the soil underneath the foundations. The seismic ground motion employed is spectrally matched with EC8 elastic spectra. This model in its linear state was validated with finite element analysis [17] and using a small scale physical experimental test at the University of Bristol's shaking table [12].

The nonlinear SSSI parametric study showed that there are significant differences in the response to the linear SSSI analysis. It is found that the nonlinear SSSI can produce a greater range of beneficial and adverse behaviour for displacement than linear SSSI, which highlights the importance of considering the nonlinear SSSI. These interaction effects increase when considering loose soil and closely spaced buildings. Here it appears that there are significant differences between the nonlinear SSSI (coupling building case) and nonlinear SSI (uncoupled building case). The most adverse effects, on building displacement, occurred when there is a big difference of height ($\varepsilon > 1.5$) between the buildings. In this case, the displacement power of building 1 can be amplified to 400%, i.e. the power of the earthquake passed from the taller structure to the small structure. In this case, nonlinear SSSI analysis indicated very large residual rotation of the buildings 1 at the end of the earthquake. This effect cannot be quantified with traditional elastic analyses and is much less significant in nonlinear SSI analysis.

For the case of a smaller building 1 (flanked by a taller building 2), the amplification in nonlinear SSSI response acceleration can be as high as 110%. Results also indicated that there is a beneficial effect for the taller building 2, with a maximum of response acceleration of -45%. This reduction does not apply for the entire range of aspect ratios.

The linear SSSI suggest that the adverse/beneficial effects boundary seems to be when building 1 and building 2 natural frequency are close. Nonlinear SSSI presents a more complex picture with interactions across a broader range of frequencies.

Results from analyses of well-spaced building, around 2 times the building base width, show that the SSSI seismic response energy amplification is negligible. For dense soil, the results show that the SSSI interaction is less relevant than for the case of loose soil.

Therefore, this paper indicates that including the presence of nonlinearity in the soil can increase the size of adverse/beneficial SSSI effects, so it should not be neglected. Additionally, there is evidence presented that suggest significant differences between nonlinear SSSI (coupled building case) and nonlinear SSI (uncoupled building case) analyses.

5. Acknowledgements

The Ministry of Education, Chile and Commission for Scientific and Technological Research (CONICYT) through grant BCH 72170305 has granted financial support to the PhD student during this research. The researchers are very grateful for the support of the Faculty of Engineering, at the University of Bristol. Most of the computations necessary for this work were carried out on the BlueCrystal supercomputers of advanced computing research centre of the University of Bristol.

References

[1] Luco JE, Contesse L. Dynamic structure–soil–structure interaction. Bull Seismol Soc Am 1973;63:1289–303.

[2] Kobori T, Minai R, Kusakab K. Dynamical characteristics of soil–structure cross-interaction system. Bull Disaster Prevent Res Inst 1973;22. Kyoto University.

[3] Lee TH, Wesley DA. Soil–structure interaction of nuclear reactor structures considering through-soil coupling between adjacent structures. Nucl Eng Des 1973;24:374–87.

[4] Mattiesen PB, MacCalden RB. Coupled response of two foundations. Proceedings of the 5th world conference on earthquake engineering. Rome, Italy; 1974.

[5] Wong HL, Trifunac MD. Two-dimensional, antiplane, building–soil–building interaction for two or more buildings and for incident planet SH waves. Bull Seismol Soc Am 1975;65:1863–85.

[6] Lysmer J, Seed HB, Udaka T, Hwang RN, Tsai CF. Efficient finite element analysis of seismic soil structure interaction. Report No. EERC 75-34. Earthquake Engineering Research Center, University of California, Berkeley, CA; 1975.

[7] Roesset JM, Gonzalez JJ. Dynamic interaction between adjacent structures. In: [C] Proceedings of dynamical methods in soil and rock mechanics, Karlsruhe, September 5–16, 1977.

[8] Kitada Y, Hirotani T, Iguch M. Models test on dynamic structure–structure interaction of nuclear power plant buildings. Nucl Eng Des 1999;192:205–16.

[9] Yano T, Naito Y, Iwamoto K, Kitada Y, Iguchi M. Model test on dynamic cross interaction of adjacent building in nuclear power plants – overall evaluation on field test, k06-2, In: Presented at the transactions of the 17th international conference on structural mechanics in reactor technology, Prague, Czech Republic, 2003.

[10] Hans S, Boutin C, Ibraim E, Rousillon P. In situ experiments and seismic analysis of existing buildings. Part I: Experimental investigations. Earthq Eng Struct Dyn 2005;34(12):1513–29.

[11] Li PZ, Hou XY, Liu YM, Lu XL. Shaking table model tests on dynamic structure- soil-structure interaction during various excitations. In: Proceedings of the 15th world conference on earthquake engineering. Lisbon, Portugal; 2012.

[12] Aldaikh H, Alexander N, Ibraim E, Knappett J. Shake table testing of the dynamic interaction between two and three adjacent buildings (SSSI). Soil Dynamic and Earthquake Engineering 2016; 89:219-232.

[13] Bard P-Y, Chazelas JL, Guéguen PH, Kham MJ, Semblat F, Site-city interaction. In: Oliveira C, Roca A, Goula X, editors. Assessing and managing earthquake risk, Springer; 2006.

[14] Yahyai M, Mirtaheri M, Mahoutian M, Daryan AS. Soil structure interaction between two adjacent buildings under earthquake load. Am J Eng Appl Sci 2008;1:121–5.

[15] Padron LA, Aznarez JJ, Maeso O. Dynamic structure–soil–structure interaction between nearby piled buildings under seismic excitation by BEM–FEM model. Soil Dyn Earthq Eng 2009;29:1084–96.

[16] Bolisetti C, Whittaker AS. Seismic structure–soil–structure interaction in nuclear power plants structures. In: SMiRT, New Delhi; 2011.

[17] Alexander NA, Ibraim E, Aldaikh H. A simple discrete model for interaction of adjacent buildings during earthquakes. Comput Struct 2013;124:1–10.

[18] Aldaikh H, Alexander NA, Ibraim E, Oddbjornsson O. Two dimensional numerical and experimental models for the study of structure-soil-structure interaction involving three buildings. ComputStruct2015;150:79–91.

[19] Pedretti S. Nonlinear seismic soil-structure interaction: analysis and modelling method [Ph.D. thesis], Politecnico di Milano, Milano, Italy, 1998.

[20] Cremer C, Pecker A, Davenne L. Cyclic macro-element for soil-structure interaction: material and geometrical nonlinearities. International Journal for Numerical and Analytical Methods in Geomechanics 2001; 25(13):1257-1284.

[21] Cremer C, Pecker A, Davenne L. Modelling of nonlinear dynamic behaviour of a shallow strip foundation with macroelement. Journal of Earthquake Engineering 2002; 6(2): 175-211.

[22] Gajan S, Thomas JM, Kutter BL. Physical and analytical modelling of cyclic load deformation behaviour of shallow foundations. 57th Annual Meeting of Earthquake Engineering Research Institute, Ixtapa, Mexico 2005.

[23] Gorbunov-Possadov MI, Serebrajanyi V. Design of structures upon elastic foundations. Presented at the 5th international conference soil mechanics foundation engineering, Paris, 1961.

[24] Bouc R. Forced Vibration of Mechanical Systems With Hysteresis. Proceedings of the 4th Conference on Nonlinear Oscillations. 1967. Prague, Czechoslovakia, p. 315.

[25] Wen YK. Method for Random Vibration of Hysteretic Systems. J. Eng. Mech. 1976, 102, pp. 249–263.

[26] Baber, TT and Wen YK. Random Vibration of Hysteretic Degrading Systems. J. Eng. Mech. 1981, 107, 1069–1087.

[27] Baber TT and Noori MN. Modelling General Hysteresis Behaviour and Random Vibration Application. ASME J. Vib., Acoust., Stress, Reliab. Des.1986, 108, 411–420.

[28] Ma F, Zhang H, Bockstedte A, Foliente GC, Paevere P. Parameter Analysis of the Differential Model of Hysteresis. Journal of Applied Mechanics. 2004;71:342-349.

[29] Ismail M, Ikhouane F, Rodellar J. The Hysteresis Bouc-Wen Model, a Survey. Arch Comput Methods Eng. 2009; 16: 161-188.

[30] Takeda T, Sozen MA, and Neilsen NN. Reinforced concrete response to simulated earthquakes. ASCE Journal of the Structural Division, 1970 96(ST12), pp. 2557-2573.

[31] Ramberg W. and Osgood WR. Description of Stress-Strain-Curves by Three Parameters. Technical Report, Technical Note No. 902, NACA, 1943.

[32] Ishibashi I, Zhang X. Unified dynamic shear moduli and damping ratio of sand and clay. Soil and Foundations. 1993;33:182-191.

[33] Tatsuoka F, Siddiquee M, Park Ch, Sakamoto M, Abe F. Modelling stress-strain relations of sand. Soil and Foundations. 1993;33:60-81.

[34] Gerolymos N, Gazetas G. Constitutive model 1-D cyclic soil behaviour applied to analysis of layered deposit. Soil and Foundations. 2005;45(3):147-159.

[35] Gerolymos N, Gazetas G. A model for grain-crushing-induced landslides – Application to Nikawa, Kobe 1995. Soil Dynamics and Earthquake Engineering. 2007;27:803-817.

[36] Drosos V, Gerolymos N, Gazetas G. Constitutive model for soil amplification of ground shaking: Parameter calibration, comparisons, validation. Soil Dynamics and Earthquake Engineering. 2012;42:255-274.

[37] Newmark NM, Rosenblueth E. Fundamentals of earthquake engineering. Prentice-Hall; 1971.

[38] Chopra AK. Dynamics of structures: Theory and applications to earthquake engineering. 2nd ed. Prentice-Hall; 2000.

[39] Clough RW, Penzien J. Dynamics of structures. 2nd ed. McGrawHill Int.; 1993.

[40] SEAOC Bluebook: The Recommended Lateral Force Requirements of the Structural: SEAOC, 1959.

[41] PEER Strong Motion Database <http://ngawest2.berkeley.edu/ >.

[42] European Standard EN 1998-1. Eurocode 8: Design of structures for earthquake resistance.

[43] Alexander NA, Chanerley AA, Crewe AJ, Bhattacharya S. Obtaining Spectrum Matching Time Series Using a Reweighted Volterra Series Algorithm (RVSA). Bulletin of the Seismological Society of America. 2014;104(4):1663-1673.

[44] Hardin B, Drnevich V. Shear modulus and damping in soils. Design equations and curves. Journal of SMFE, Proc. Of ASCE. 98:667-692.

[45] Chatfield C, The Analysis of time Series: An introduction, Six Edition, 2003 by Chapman and Hall/CRC.

[46] Aldaikh H, Alexander NA, Ibraim E, Knappett J. Evaluation of rocking and coupling rotational linear stiffness coefficient of adjacent foundations. International Journal of Geomechanics (accepted 2017).

[47] Chouw N, Schmid G. Influence of geometrical effects of the soil on structure-soil-structure interaction. In w.B Kratzig et al (eds,), Structural Dynamics, A.A. Balkema, Rotterdam, pp 795-802.

[48] Ogut OC, Fukuwa N. In-plane dynamic behaviour of two adjacent buildings focused on different embedment depths and foundation types. Journal of Structural and Construction Engineering (Transactions AIJ) 2017; v82, 734:521-531.

[49] MATLAB. The Mathworks, Inc. version R2016a.

[50] Trombetta NW, Hutchinson TC, Mason HB, Zupan JD, Bray JD, Bolisetti C, et al. Centrifuge modeling of structure–soil–structure interaction: seismic performance of inelastic building models. In: Presented at the 15th world conference on earthquake engineering, Lisbon, Portugal; 2012.

[51] Trombetta NW, Mason HB, Chen Z, Hutchinson TC, Bray JD, Kutter BL. Nonlinear dynamic foundation and frame structure response observed in geotechnical centrifuge experiments. Soil Dyn Earthq Eng 2013;50: 117–33.

[52] Trombetta NW, Mason HB, Hutchinson TC, Zupan J., Bray JD, Kutter BL. Nonlinear Soil-Foundation-Structure and Structure-Soil-Structure Interaction: Engineering Demands. J. Struct. Eng. 2015;141(7).

[53] Mason HB, Trombett NW, Chen Z, Bray JD, Hutchinson TC, Kutter BL. Seismic soil–foundation–structure interaction observed in geotechnical centrifuge experiments. Soil Dyn Earthq Eng 2013;48.

[54] Ghandil M, Behnamfar F. Dynamic responses of structure-soil-structure systems with an extension of the equivalent linear soil modelling. Soil Dyn Earthq Eng 2016;149-162.

[55] Botisetti C, Whittaker A. Structure-Soil-Structure interaction. Transaction, SMiRT-23, 2015. Manchester, UK.

[56] European commission EUR 23563 EN-2008. A review of the seismic hazard zonation in national building codes in the context of Eurocode 8.